

Airflow modelling studies over the Isle of Arran, Scotland

J. Thielen[†] and A. Gadian[†]

Physics Department, UMIST, Manchester M60 1QD, UK

S. Vosper[†] and S. Mobbs[‡]

School of Environment, University of Leeds, Leeds, UK

Abstract. A mesoscale meteorological model is applied to simulate turbulent airflow and eddy shedding over the Isle of Arran, SW Scotland, UK. Under conditions of NW flow, the mountain ridge of Kintyre, located upwind of Arran, induces gravity waves that also affect the airflow over the island. The possibility to nest domains allows description of the airflow over Arran with a very high resolution grid, while also including the effects of the surrounding mainland of Scotland, in particular of the mountain ridge of Kintyre. Initialised with a stably stratified NW flow, the mesoscale model simulates quasi-stationary gravity waves over the island induced by Kintyre. Embedded in the larger scale wave trains there is continuous development of small-scale transient eddies, created at the Arran hill tops, that move downstream through the stationary wave field. Although the transient eddies are more frequently simulated on the northern island where the terrain is more pronounced, they are also produced over Tighvein, a hill of 458 m on the southern island where measurements of surface pressure and 2 m meteorological variables have been recorded at intermittent intervals between 1996 and 2000. Comparison between early observations and simulations so far show qualitatively good agreement. Overall the computations demonstrate that turbulent flow can be modelled with a horizontal resolution of 70 m, and describe turbulent eddy structure on wavelength of only a few hundred metres.

Key words: rotors; reverse flow; high resolution; modelling over steep terrain.

1. Introduction

Hills represent an obstruction to the airflow and may produce waves, shedding eddies, clouds, and other turbulent phenomena in the lee of the hill tops (e.g., Carruthers and Hunt 1990, Banta 1995). Under certain meteorological conditions the turbulence can become so severe that it represents a hazard to air traffic. A well-known example for this is Hong-Kong International airport where a combination of gravity waves and mechanically generated turbulence induced by the hills on Lantau island produce not only turbulence (Neilley *et al.* 1995) but also strong wind shear (Lau and Shun 2000) making take-off and landing a difficult and dangerous task.

The effects of hills on airflow have been studied in great detail over the past decades, however, mostly under idealised conditions. For example, many studies are based on simplified topographies such as isolated hills (e.g., Clark 1977, Mason and Sykes 1979, Smith 1980). Substantial work on

[†] Ph.D.

[‡] Professor

the subject has been performed by Hunt and Carruthers (1990) who investigated the flow and the turbulence characteristics both for idealised as well as for complex terrain under different scenarios of stratification and Froude numbers. Many of the studies have given great insight and understanding of the different processes involved in the development of lee waves, eddy shedding, and turbulent wake structures. Smith (1989) for example found that splitting of the flow around mountains occur when a stagnation point exists and when the Froude number is sufficiently small. Idealised studies cannot, however, capture all the turbulent processes at a certain site in their full complexity. Baines (1995) found for example that asymmetric shaped mountains are almost certainly associated with unsteady wakes and shedding eddies which cannot be described within a simplified framework.

Therefore the development of the atmospheric phenomena need to be studied carefully in relation to the particular topography and meteorological conditions : observations of variables such as wind, temperature, pressure, or turbulence need to be made on site with a high density gauge network or remote sensing techniques and modelling studies need to include the full description of the terrain and the meteorological conditions. Rasmussen *et al.* (1989), for example, applied a 3D mesoscale model to the island of Hawaii allowing him for the first time to show the eddy shedding and wake downwind of the island. Shutts and Broad (1993) simulated the effect of the Pennines on the development of lee waves. Comparison with observations confirmed that amplitude and phase of the lee waves was well predicted by their model.

Another important finding of Clark *et al.* (1997) has advanced the research of turbulent flows in complex terrain. Following the field study in Neilley (1995), they applied a 3D non-linear and non-hydrostatic mesoscale meteorological model to Lantau island to simulate the development of turbulent airflow at Hong Kong International airport using different grid resolutions. Their results show considerable differences in the solutions for 250, 125 or 62.5 m. Only with a high grid resolution below 100 m did the model describe certain turbulent features correctly. Due to computing limitations, however, the necessary high resolutions are often not easy to achieve.

The objective of this paper is to study the near-surface airflow generated over complex terrain and under influence of gravity waves using a non-linear meteorological model. As a case study, the Isle of Arran is chosen. The topography of Arran is complex and in the North dominated by sharp and steep mountains up to 900 m high; in the South the topography consists of rolling hills (maximum heights around 500 m). Significant topography lies only a few tens of kilometres to the North and West of Arran (Fig. 1) and thus the airflow impinging on the island is unaffected by upstream mountains for southerly or south-westerly winds only. For other wind directions, one might expect the flow over Arran to be modified by the upstream topography. Gravity waves are the dominant contributor to the drag since usually $U/NL < 1$ where U is the wind, N is the buoyancy frequency at hill height H , and L is the hill width. In this case the gravity waves are likely to interact with the flow over the island. A grid-nesting procedure (Clark and Farley 1984) is used allowing the Isle of Arran to be resolved with a grid spacing of 70 m, and the surrounding mainland of Scotland with 250 m.

Several field campaigns have taken place within the period of 1996-2000 to study the airflow over Arran measuring surface pressure and 2 m-temperature (Vosper *et al.* 2000). Turbulence has also been measured at a few sites. Most of the observation sites are concentrated on the southern part of the island. From December 1999 to April 2000, an extensive field campaign has been conducted with more than 40 masts placed over the Southern Isle; these data are now being analysed. For NW flow surface observations and aircraft measurements suggest that the pressure field due to gravity waves generated by Kintyre and the mountains in the very North of Arran itself, may effect the flow in the

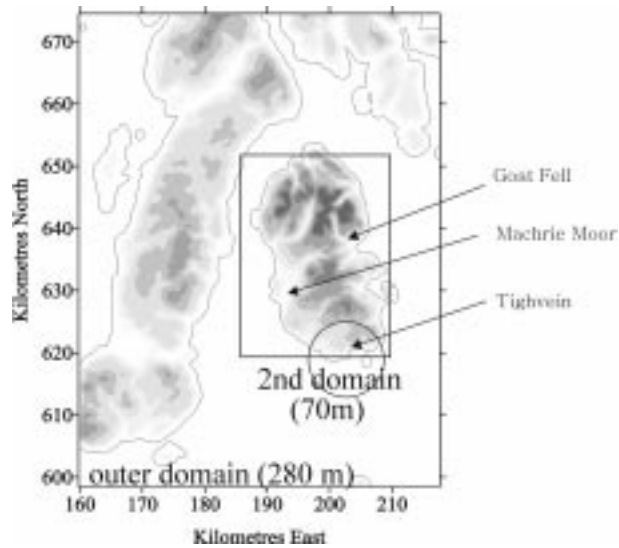


Fig. 1 Illustration of the model set-up including topography and positioning of domains. The axes are labelled in National Grid coordinates in km E in x -direction and km N in y -direction. The circle highlights the area around hill Tighvein on which the case study is focused. Machrie Moor is the position of the radiosonde launches. For reference the exact position of hill Tighvein and Goat Fell are also indicated

boundary layer over Tighvein, with 458 m the highest hill on the southern island. The observational data suggest that two types of flow separation on Tighvein exist: (i) flow splitting with air flowing around the hill rather than over the hill and (ii) flow splitting during phases of unsteady eddy shedding in the lee of the hill with local flow reversal. When (ii) was observed, the eddy shedding was always accompanied by prolonged periods of reversed, i.e., upwind, drag. A possible explanation for the reversed pressure drag is that the local pressure field is influenced by gravity wave field.

The Arran case study is preparatory to another field study on the Falkland Islands, where similar geographical conditions as on Arran produce severe wind storms and turbulence that represent a great hazard to aviation on Mount Pleasant airport. The overall aim of the project is to construct a linear model that allows to predict an increased likelihood for the development of severe turbulence and winds storms 10-12 hours ahead in order to alleviate hazards or damage associated with these events. Linear models, well capable of describing the gravity wave fields induced by terrain (Vosper *et al.* 2000) cannot, however, simulate the turbulent eddies in detail. They need to be studied within a non-linear numerical framework.

The non-linear model and its set-up are briefly described in Section 2 and Section 3. In section 4, results of observations of the 1998 field campaign and the high-resolution simulations are shown, both illustrating the development of reverse flow zones. Conclusions are drawn in Section 5.

2. Description of the model

In this study the dynamical cloud resolving model developed by Clark and others (Clark 1977, Clark and Farley 1984, Clark and Hall 1991, 1996) is applied. It has been used to simulate a wide range of mesoscale atmospheric processes including flow over complex terrain (Clark and Gall 1982, Clark *et al.* 1997) and eddy shedding (Rasmussen *et al.* 1998).

The model is a finite-difference approximation to the anelastic, non-hydrostatic time-dependent Navier-Stokes equations, including the effects of moisture. The system variables are expanded around profiles of an idealised atmosphere with constant stability. Thermodynamic variables are described by conservation equations of heat and moisture. The finite difference formulation uses a second order algorithm for the conservation of momentum, and a second order accurate, positive-definite advection transport algorithm of Smolarkiewicz (1984) for the conservation of all thermodynamic variables. A second-order leapfrog scheme is used for the time derivatives.

In the horizontal, the grid is cartesian, and in the vertical the model uses a terrain influenced coordinate system based on Gal-Chen and Somerville (1975) such that the lowest grid points of the model are aligned with the terrain, and the top is at a constant level. The variables are distributed on an Arakawa-C scheme. The model uses a two-way interactive grid nesting (Clark and Farley 1984).

Subgrid scale turbulent processes are parameterised using a first order closure of Lilly (1963) and Smagorinsky (1963). At the lower boundary, a drag law describes the effects of surface friction. In the atmospheric boundary layer, stress is a function of the eddy mixing coefficient, K , and the velocity field. Within the surface boundary layer, K is a function of deformation, above the surface layer K is mainly a function of the Richardson number (Thielen *et al.* 2000). Parameterisation of the microphysical processes is based on the schemes of Kessler (1969) for warm rain, and of Koenig and Murray (1974) for ice.

In order to damp 2d-waves in either x - or y -direction, a spatial horizontal filter of the order ∇^6 is employed at the interior of the domain on deviations of the wind components and thermodynamic variables from their environmental averages during each time step. For more detail on the filters, the reader is referred to Clark (1977).

3. Model set-up

The model is set-up with two nested domains (Fig. 1). The outer domain extends 60 km in East/West and 74 km in North/South directions, and includes the Isle of Arran as well as the mainland to the NW. The grid resolution is 280 m in the horizontal and the vertical. The second domain covers the Isle of Arran only, with a resolution of 70 m in the horizontal and the vertical. With this high resolution, the topography data needed to be smoothed to avoid numerical instabilities. The highest elevation is located on Arran at Goat Fell with 875 m.

The initialisation profile, measured on March 13, 1998, from Machrie Moor on Arran shows NW winds and a stable stratification of the atmosphere (Fig. 2). A particularly stable lid is present at the top of the boundary layer at 800 hPa. On this day, visible wave activity was observed over Arran, as well as some flow separation on the southern part of the island. The time step is 6 seconds in the outer domain and 1 second in the inner domain. The mesoscale model is run for 90 min with the outer domain only before the inner domain is ‘spawned in’. A period of 10 minutes is allowed after the spawning to ensure that the flow in the inner domain is adjusted; this method allowing the saving of computing time. The flow in the inner domain is then simulated for a further 30 minutes, during which data is output every 1 minute. The lower boundary condition is free-slip with surface friction formulation.

4. Results

4.1. Observational results

From 1996 to 2000 a number of observational field campaigns have been carried out on Arran.

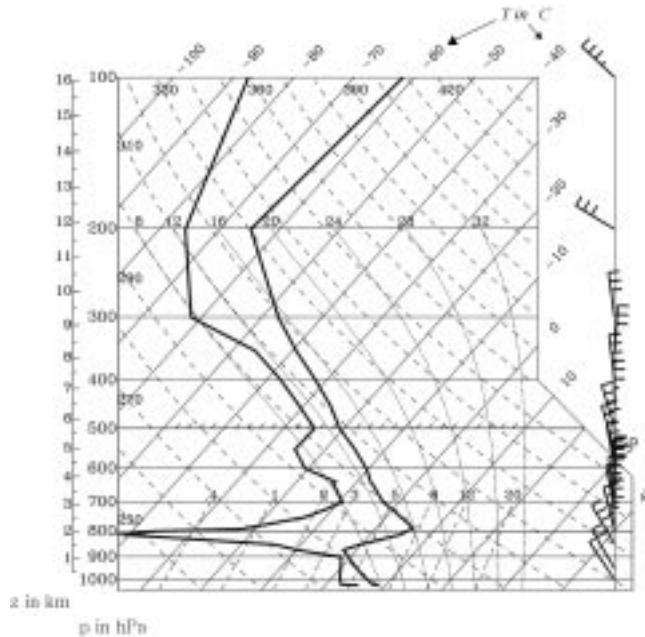


Fig. 2 Skew-T diagram of March 13, 1998, 11 am, the profile used to initialise the model. Profiles of temperature and humidity can be plotted on a Skew-T thermodynamic diagram. Pressure levels and height are shown on the left hand side of the diagram in hPa and km respectively. Temperature and dew point temperature are outlined, the corresponding axis being the diagonal solid lines, labelled on the right hand side and the top of the diagram in °C. The winds are shown as barbs in m/s on the right hand side, one long horizontal dash representing 10 m/s, and triangles representing 50 m/s

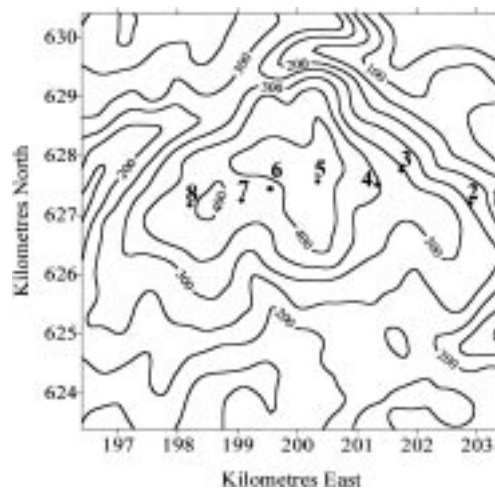


Fig. 3 Height contours in the vicinity of hill Tighvein and the position of 8 measuring sites across the summit. The axes are labelled in Ordnance Survey reference as in Fig. 1

Except for the last campaign (December 1999 to April 2000) for which the data sets are presently being prepared. The early experiments consisted of a few masts across hill Tighvein measuring pressure,

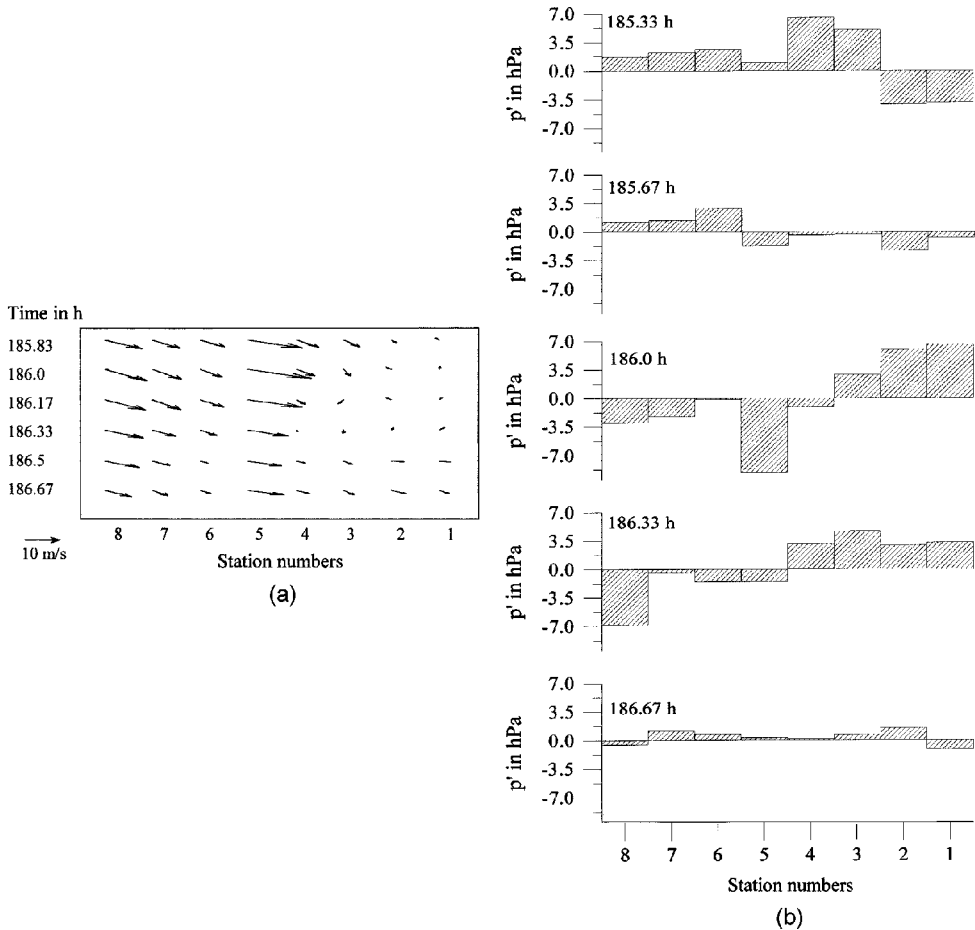


Fig. 4 (a) The top diagram shows the evolution of the 10-min averaged 2 m winds measured at 8 stations across hill Tighvein on 13 March 1998. The time is given in hours since the start of the field experiment. Station numbers correspond to the locations in Fig. 3. (b) The bottom diagram illustrates the evolution of the 10 min-average pressure deviation p' measured at the 8 stations across hill Tighvein. Time and station numbers are given as in top diagram

winds and temperature for 10 min averages only. Fig. 3 illustrates the topography around hill Tighvein and the position of 8 masts along a East/West transect where measurements of 2 m wind, temperature and surface pressure were made for periods of several weeks during 1997 and 1998. Fig 4a shows the evolution of the measured 10-minute averaged 2 m wind on 13 March 1998. There is a clear speed-up of the wind over the hill top with deceleration on the lee slope. From 186 hours onwards the data shows that a reversed flow is sustained for a 40-min period 3 km east of Tighvein's summit (stations 1, 2 and 3). The observational data suggest that the reversed flow may be caused by a single eddy about 1.5 km in diameter growing from East to West. Although periods of reversed flow were recorded throughout the field campaigns, they appear to occur rather infrequently and are usually short lived. This may be because the data were recorded as 10 minute averages; higher temporal resolution might have revealed more events. In all the observed cases of flow reversal on

the lee slope of Tighvein in NW flow, there appears to be a reversed pressure drag across Tighvein i.e., low pressure (after removal of the component due to the height differences of the instruments) is located on the upwind slope with high pressure on the lee slope, as illustrated in Fig. 4b.

As can be seen from Fig. 4a, the pressure reversal coincides temporally with the observed reversed flow. It seems plausible that such a locally reversed pressure field could be imposed by the gravity waves generated upstream of Tighvein. Hence, a slight shift in phase of the waves (due to wave unsteadiness or changes in the synoptic flow) could completely alter the pressure field on Tighvein and thus influence the regions of reversed flow on the lee slope. Analysis of the synoptic surface pressure on that day shows a sudden pressure drop followed by a rise about one hour prior to the development of the eddy. Although this suggests the passage of a weak front, this cannot be confirmed because of the lack of other observational data. In conjunction with the very stable layer at the top of the boundary layer, this could have created favourable conditions for a temporary gravity wave enforcement leading eddy development.

Although the data is clearly suggestive, the conclusion about the nature of the reversed flow cannot be drawn with certainty. It is possible, for example, that the wind arrows do not illustrate a single closed eddy, but a temporary modified flow pattern with more air pushing around hill Tighvein from the West. In order to obtain more information on the flow regime, the mesoscale meteorological model has been initialised with the radiosonde profile from March 13, 1998, 11 a.m. Apart from simulating the turbulent motion and shedding eddies in the lee of the hill tops over the whole of Arran, its results are also used to ‘fill the gaps’ left by the observations on Tighvein.

4.2. Modelling results

As an implication of the two-way interactive nesting, strictly speaking, only the high-resolution inner domain produces valid results. Therefore, in the following, the analysis is restricted to the second model domain.

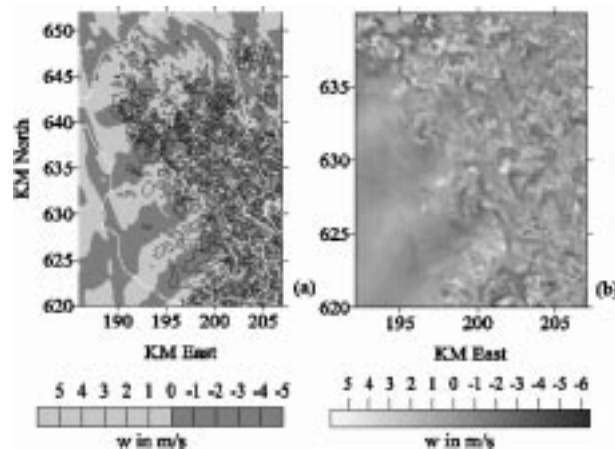


Fig. 5 On the left, a horizontal slice through the vertical velocity field in the inner domain at a height of 910 m after 100 min of simulation (a). The slice is illustrated as a contour plot. Negative values are shaded dark grey, positive values light grey. The contours are regularly spaced in 1 m/s intervals. The coast of the island is outlined in white. On the right, a shaded zoom of the SE corner of Fig. 5a is shown as shaded surface plot (b). An imaginary light source is situated in the NW, and crests are shaded white and valleys dark

As a first overview over the atmospheric processes, Fig. 5a shows a horizontal slice through the second domain of the vertical velocity at 910 m a.s.l., just above the highest elevation peak in the North of the island, Goat Fell (875 m), at 100 min of simulation. Negative values are illustrated with dark grey, positive values as light grey. Contours are drawn in 2 m/s intervals from -5 m/s upwards. The outline of the Isle of Arran is also illustrated with a white line. Obviously, there is a clear gravity wave signature in w , with a horizontal wavelength of about 7 km. The wave field remains steady during the 30 min of high-resolution modelling. However, downwind of the high elevation terrain in the North of the island, the flow becomes increasingly turbulent, and SW of Goat Fell the gravity waves are split into two wave trains, with the phase of the eastern wave train slightly ahead of that to the West. Using a linear model technique, the same gravity wave structure, including the gap, is also found (Thielen *et al.* 2000). The mesoscale model results show that the flow in the gap between the two waves is quite turbulent. Fig. 5b is a shaded surface plot and shows a zoom of the SE of the second domain. It illustrates the complex and highly turbulent structure of the flow over the Isle embedded in the gravity wave trains. The summit of Tighvein is located within this ‘wave gap’. Animation of the temporal development of the fields can be seen under

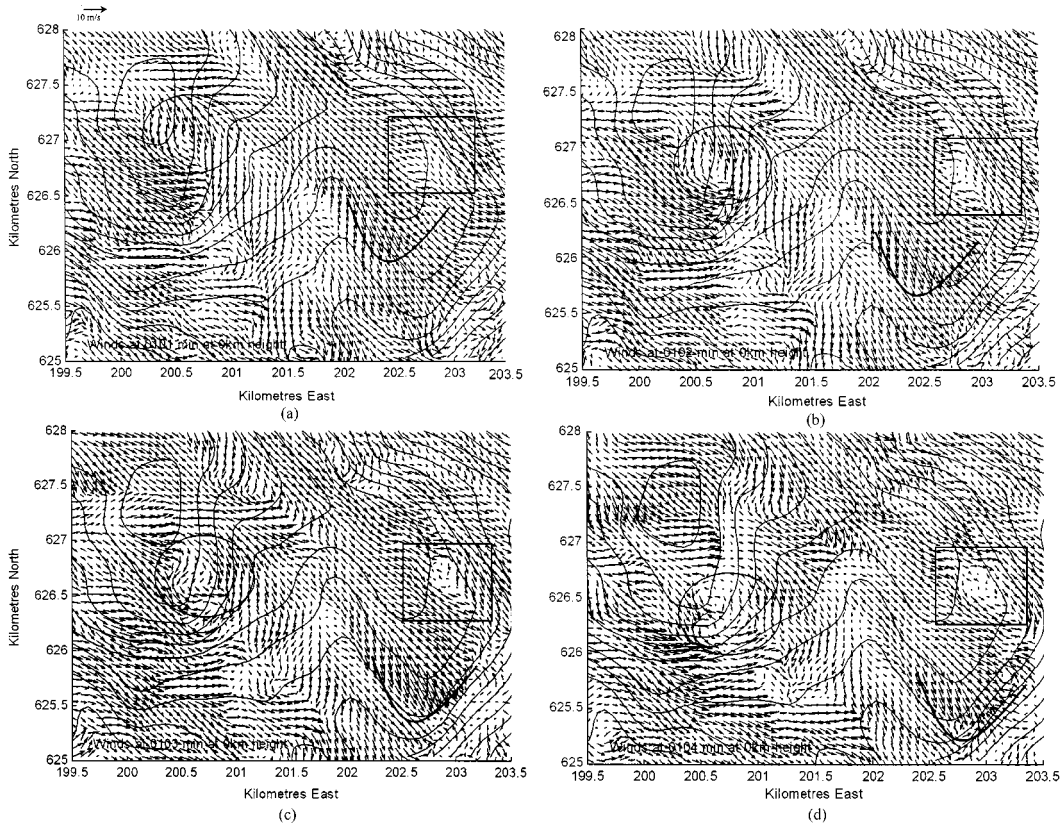


Fig. 6 a-d: xy -plot of the surface winds 101 min (a), 102 min (b), 103 min (c) and 104 min (d). The x - and y axis are Kilometres East and North respectively. The circle highlights the propagation of an eddy moving downwind until being absorbed by a wake street leeward of hill Tighvein. The square highlights the position of a recirculation zone that lasts in total for about 10 min. The front edge of a gustfront moving south is highlighted by a v -shaped line

<http://atmos.phy.umist.ac.uk/arran>. The animations illustrate propagating eddies that are not observed when the model is run with 1 domain only and a grid resolution of 280 m. This stresses the importance of the high resolution and the necessity of nested domains.

At the surface, the flow is equally turbulent as illustrated in Fig. 6. The focus of analysis is on the airflow around hill Tighvein. Figs. 6a-c illustrate the development of the horizontal surface winds from 101 to 104 min in 1 min intervals for the inner region outlined in Fig. 3. The figure shows nicely the wakes downwind of the hill, the regions of stagnant flow, rapidly moving transient eddies as well as persistent recirculation zones.

In particular 3 different zones are highlighted in Fig. 6, (A) a circle highlighting an eddy originating on top of Tighvein and moving downwind, (B) a V-shaped hook illustrating the front-edge of a gust-front, and (C) a square highlighting another eddy lasting for about 10 min, roughly at the same location as the observed reversed flow (Fig. 3).

- (A) The eddy shedding on top of hill Tighvein moves rapidly downwind and merges with a clearly visible wake street in the lee of the hill. Comparison between the development of the pressure (Figs. 7a-d) and the wind field at the surface suggests that this eddy is directly associated with the pressure field around Tighvein. At 102 min the pressure perturbation distribution still shows the expected positive p^{**} upwind of the summit and negative p^{**} downwind of the summit. In subsequent time steps, however, the ‘pocket’ of negative pressure moves downwind. The wind field is clearly influenced by the pressure field keeping a tendency to flow towards the low pressure.
- (B) The V-shaped hook illustrates the front edge of a gust front moving southward from the top of the ridge. This gust is created by an vertical eddy producing downdraughts of the order of

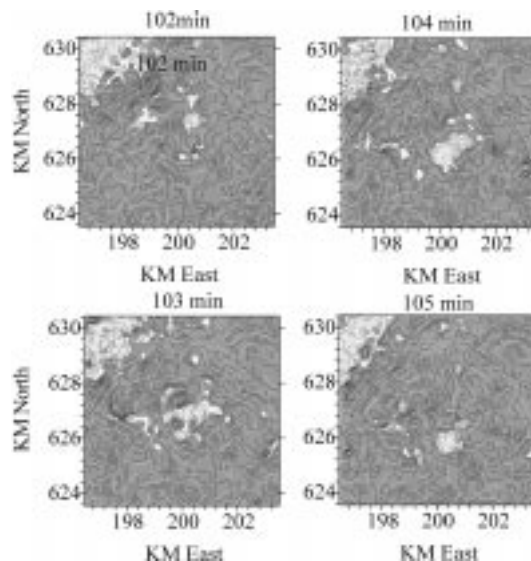


Fig. 7 Mesoscale model surface pressure perturbation field, $p^{**} = p - p_{\text{syn}} - p_{\text{hydro}}$ (the time dependent component of the pressure after the synoptic and hydrostatic components have been removed), around hill Tighvein (summit at 200 kmE, 627.3 kmN) at 102, 103, 104, and 105 min. The x - and y axis are given in Kilometres East and North respectively. The topography is outlined in white contours in 50 m steps. Negative pressure is shaded light grey, positive pressure is shaded dark grey. The contours are regularly spaced with 0.05 hPa.

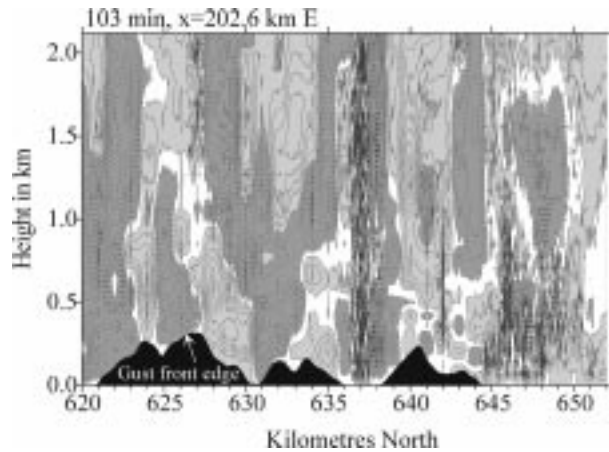


Fig. 8 YZ-cut of the vertical wind component at $x = 202.6$ km East at 103 min. Updraughts are shown as light grey and are contoured with solid lines in 0.25 m/s intervals. Negative values are shown in dark grey with dashed contour lines, also in 0.25 m/s intervals. The topography is shaded black. The aspect ratio of domain height to domain length is greatly exaggerated. The y-axis is height in km, the x-axis km North

6 m/s instead of the average 2-3 m/s at the surface. Fig. 8 shows a YZ-cut of the vertical wind component at $x = 202.6$ km East at 103 min. Updraughts are shown as light grey and are contours with solid lines in 0.25 m/s intervals. Negative values are shown in dark grey with dashed contour lines, also in 0.25 m/s intervals. The topography is shaded black. The aspect ratio of domain height to domain length is greatly exaggerated. This figure illustrates the wave structure characterised by alternating regions of up- and downdraughts throughout the domain imposed by the gravity wave from 1 km height upward. Closer to the surface terrain, induced modifications of the flow become apparent, in particular around the higher hill tops, e.g., around 635 and 630 km E. The gust front illustrated in Fig. 6 is induced by the compensating downdraught between two updraught regions.

- (C) The square highlights a region of stagnant and reversed flow East of the summit. This recirculation zone is simulated at the same location where the sustained eddy is observed during the field campaign (186.13 h on 13 March 1998, see Fig. 2). The recirculation starts at about 101 min at 202.6 km E, 626.75 km N, is strongest at 103 min, and moves downstream while weakening from 105 min onwards (not shown). In total, the eddy lasts for about 10 minutes and has an average diameter of about 500 m. Thus, although located at the same place, this eddy is not as intense or as long lived as the observed one (Fig. 3). The surface pressure perturbation field is weak at this location. Analysis of the temporal development of the three wind components shows that the approaching reversed flow in the horizontal is associated with the weakening of a previously strong downdraught, which changes sign at the time the eddy passes, the vertical flow at the surface becoming slightly positive (Fig. 9). It is possible that the orography plays an important role in the formation of the eddy at this location, instead of, for example a gust front.

It is hoped that the data from the new field campaign that has recently been conducted on Arran employing a high-density network of surface-based instruments and further modelling will provide further insight into these flows.

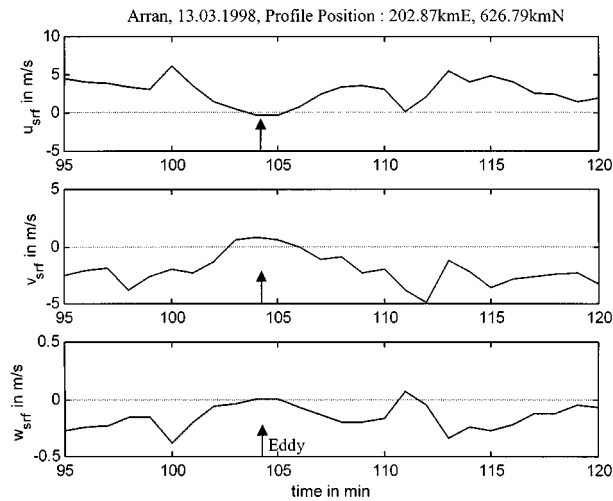


Fig. 9 Temporal development of the three wind components u , v , and w at the surface at location 202.87 km E, 626.79 km N. The y -axis is shown in m/s for all wind components, the x -axis in minutes of simulation. The time when the eddy passes the location is illustrated by an arrow in all three plots.

5. Conclusions

A 3D mesoscale meteorological model is applied to simulate near-surface turbulent airflow and eddy shedding over the Isle of Arran, SW Scotland, UK. Under conditions of NW flow, the mountain ridge of Kintyre, located upwind of Arran, induces gravity waves that also affect the airflow over the island. The model is used with the grid-nesting option allowing to capture the larger scale flow including Kintyre with a relatively coarse resolution of 250 m, and to telescope into the area of interest, the Isle of Arran, with a comparatively much high grid-resolution of 70 m. The model is set-up for stable condition observed on March 13, 1998. On this day, gravity wave clouds were observed and analysis of 10 min average data of winds and pressure suggest that prolonged periods of reverse flow occurred on that particular day.

Model results and surface observations suggest that gravity waves developing in the lee of Kintyre influence the boundary-layer airflow over the southern part of the Isle of Arran. In particular, when wave train splitting leeward of important terrain occurs, those areas located in the ‘wave train gap’ experience transient pressure anomalies that also influence the surface flow. Under stably stratified NW flow, two types of flow splitting are simulated: (i) low-level flow splitting gives rise to the continuous production of wake vortices and (ii) transient eddies shedding at the summit produce small-scale, short-duration episodes of flow reversal downwind of the hill tops.

Acknowledgements

The authors would like to thank all those involved in making the field measurements, in particular the colleagues from the University of Leeds, the UK Forestry Commission, the UK Meteorological Office, the British Antarctic Society and Mr. Martin Hill of Holtech Associates. The authors would also like to acknowledge the financial support of the Ministry of Defence.

References

- Baines P.G. (1995), *Topographic Effects in Stratified Flows*, Cambridge Univ. Press, 421.
- Banta, R.M. (1990), "The role of mountain flows in making clouds. Atmospheric processes over complex terrain", Monographs, (Ed. W. Blumen), Met. Monogr., AMS, **23**, Number 45.
- Carruthers, D.J. and Hunt, J.C.R. (1990), "Fluid mechanics of airflow over hill: turbulence, fluxes, and waves in the boundary layer", *Atmospheric Processes over complex terrain* (Chapter 5), AMS (1990).
- Clark, T.L. (1977), "A small-scale dynamic model using a terrain following coordinate transformation", *J. Comp. Phys.*, **24**, 186-215.
- Clark, T.L. and Farley, D. (1984), "Severe downslope windstorm calculations in two and three spatial dimensions using anelastic interactive grid nesting: a possible mechanism for gustiness", *J. Atm. Sci.*, **41**, 329-350.
- Clark, T.L. and Gall, R. (1982), "Three-dimensional numerical simulations of airflow over mountainous terrain: a comparison with observations", *Mon. Weath. Rev.*, **110**, 766-791.
- Clark, T.L. and Hall, W. (1991), "Multi-domain simulations of the time dependent Navier-Stokes equations.: Benchmark error analysis of nesting procedures", *J. Comp. Physics*, **92**, 456-481.
- Clark, T.L. and Hall, W.D. (1996), "On the design of smooth, conservative vertical grids for interactive gridnesting with stretching", *J. Appl. Meteor.*, **35**, 1040-1046.
- Clark, T.L., Keller, T., Coen, J., Neilley, P., Hsu, H., and Hall W.D. (1997), "Terrain induced turbulence over Lantau Island", *J. Atm. Sci.*, **54**, 1795-1814.
- Gal-Chen T. and Somerville R.C.J. (1975), "On the use of a coordinate transformation for the solution of the Navier-Stokes equation", *J. Comp. Phys.*, **17**, 209-228.
- Kessler, E. (1969), "On the distribution and continuity of water substance in atmospheric circulations", *Meteor. Monogr.*, **32**, p84.
- Koenig, L.R. and Murray, F.W. (1976), "Ice-bearing cumulus cloud evolution, numerical simulation and general comparison against observation", *J. Appl. Meteor.*, **15**, 747-762.
- Lau, S.Y. and C.M. Shun (2000), "Observation of terrain-induced windshear around Hong Kong International Airport under stably stratified conditions", *Proc. of 2000 9th Conf. on Mountain Meteor.*, Aspen, Colorado, USA, Aug. 7-11, Amer. Met. Soc., 93-98.
- Lilly, D.K. (1963), "On the numerical simulation of buoyant convection", *Tellus*, **14**, 145-172.
- Mason, P.J. and Sykes, R.J. (1979), "Flow over isolated hill of moderate slope", *Quart. J. Roy. Met. Soc.*, **105**, 383-395.
- Neilley, P.P., Foote G.B., Clark, T.L., Cornman, L.B. Hsu, H., Keller, J. and Rodi, A.R. (1995), "Observations of terrain induced turbulent flows in the wake of mountain islands", *7th Conf. On Mountain Meteorology, Breckenridge, Colorado*, American Meteorological Society Publication, 264-269.
- Rasmussen R.M., Smolarkiewicz P.K., and Warner, J. (1989), "On the dynamics of Hawaiian cloud bands: comparison of model results with observations and island climatology", *J. Atm. Sci.*, **46**, 1589-1608.
- Shutts, G. and Broad, A. (1993), "A case study of lee waves over the lake district in Northern England", *Quart. J. Roy. Met. Soc.*, **119**, 337-408.
- Smagorinsky, J. (1963), "General circulation experiments with primitive equations", *Mon. Wea. Rev.*, **91**, 99-164.
- Smith, R.B. (1989), "Hydrostatic airflow over mountains", *Adv. In Geophys.*, **31**, 1-41.
- Smolarkiewicz, P.K. (1984), "A fully multi-dimensional positive definite advection transport algorithm with small implicit diffusion", *J. Comp. Phys.*, **54**, 325-362.
- Thielen, J. and Gadian, A. (1996), "Influence of different wind directions in relation to topography on the outbreak of convection in Northern England", *Ann. Geophysicae*, **14**, 1078-1087.
- Thielen J., A. Gadian, S. Vosper and S. Mobbs (2000), "Simulation of transient eddies and flow separation over the Isle of Arran", *Proc. of 2000 9th Mountain Meteor. Conf.*, Aspen, Colorado, USA, Aug. 7-11, 89-92.
- Thielen J., Wobrock W., Mestayer P., Creutin J.-D., and Gadian A. (2000), "The influence of the lower boundary on convective rainfall development; a sensitivity study", *Atm. Res.*, **54**, 15-39.
- Vosper, S.B. and Mobbs S.D. (1996), "Lee waves over the English Lake District", *Q. J. Roy. Met. Soc.*, **122**, 1283-1315.
- Vosper S., A. Doernbrack, S. Eckermann and K. Carslaw (2000), "A numerical model for lee wave forecasting", *Proc. of 2000 9th Conf. On Mountain Meteorology*, Aug. 7-11, Aspen, Colorado, Amer. Met. Soc., 417-422.